Performance of the QWIP Focal Plane Array for NASA's Landsat 9 Mission

M. Hickey[a], N. Boehm[e], R. Foltz[a], Em. Kan[a], M. Montanaro[b], S. Cheung[c], B. Cho[c], C. Del Cid[c], M. Jhabvala[a], C. Tucker[c], M. Sansebastian[d], F. Wang[c], N. Costen[f], and G. Manos[a]

[a]NASA Goddard Space Flight Center, 8800 Greenbelt Road, Greenbelt, MD 20771, USA
[b]Rochester Institute of Technology, 1 Lomb Memorial Drive, Rochester, NY 14623, USA
[c]Arctic Slope Regional Corporation Research and Technology Solutions, 6303 Ivy Lane, Suite 130, Greenbelt, MD 20771, USA
[d]Conceptual Analytics, LLC, 8209 Woburn Alley Road, Glenn Dale, MD 20769, USA
[e]Global Science and Technology, 7855 Walker Drive, Suite 200, Greenbelt, MD 20770, USA
[f]SGT, Inc. Headquarters, 7701 Greenbelt Road, Suite 400, Greenbelt, MD 20770, USA

ABSTRACT

The flight focal plane array (FPA) for the Thermal Infrared Sensor 2 (TIRS-2) instrument, to be flown on Landsat 9, was built and characterized at NASA Goddard Space Flight Center (GSFC). The FPA was assembled using GaAs quantum well infrared photodetector (QWIP) arrays from the same lot as the TIRS instrument on Landsat 8. Each QWIP array is hybridized to an Indigo ISC9803 readout integrated circuit (ROIC) with 640 x 512, 25μm by 25μm pixels. Each QWIP hybrid was tested at the NASA/GSFC Detector Characterization Laboratory (DCL) as a single sensor chip assembly (SCA). The best SCAs in terms of performance were then built up into an FPA consisting of three SCAs, required to provide the necessary 15-degree field of view of the instrument. The FPA was tested to determine if project requirements were being met as a fully assembled unit. The performance of the QWIP SCAs and the fully assembled, NASA flight-qualified FPA will be reviewed.

Keywords: QWIP, Quantum Well Infrared Photodiode, Landsat 9, FPA, Focal Plane Array, Focal Plane, Infrared Detector, GaAs Detectors, Thermal Infrared Sensor, Thermal Infrared Sensor 2

1. INTRODUCTION

The TIRS-2 flight FPA was assembled and tested at NASA GSFC's Detector Characterization Laboratory using excess SCAs and parts from TIRS-1. The TIRS-2 flight FPA design was identical to the TIRS-1 design.[1] The QWIP SCAs were initially selected based on TIRS-1 test results.[2] Of the four selected, all were retested as SCAs and it was confirmed that their characteristics had not changed. The three most similar SCAs (in terms of spectral shape) were selected and built up into the flight FPA. The fully assembled FPA was tested at the DCL to determine whether it met project requirements. A summary of these results is presented here.

2. REQUIREMENTS

The TIRS-2 FPA requirements are identical to the TIRS-1 FPA requirements.[3] The layout of the FPA can be seen in Figure 1. Each of the three SCAs have 640 by 512, 25μm square pixels. The FPA layout has an overlap of 27 columns for detectors 'A' and 'C' as well as detectors 'B' and 'C'. The left-most eight columns of detector 'A' and right-most eight columns of detector 'B' are ignored. This leaves a total of 1850 pixel columns combining all three hybrids which will cover the 185 kilometer swath width (100m per pixel). Of the 512 total rows, only six will be read out from each of the hybrids. Of the six rows read out, two will be used for each of the three bands (dark, 10.8μm, and 12.0μm).

Further author information: Send correspondence to Michael R. Hickey
E-mail: michael.hickey@nasa.gov, Telephone: 1 301 286 3833

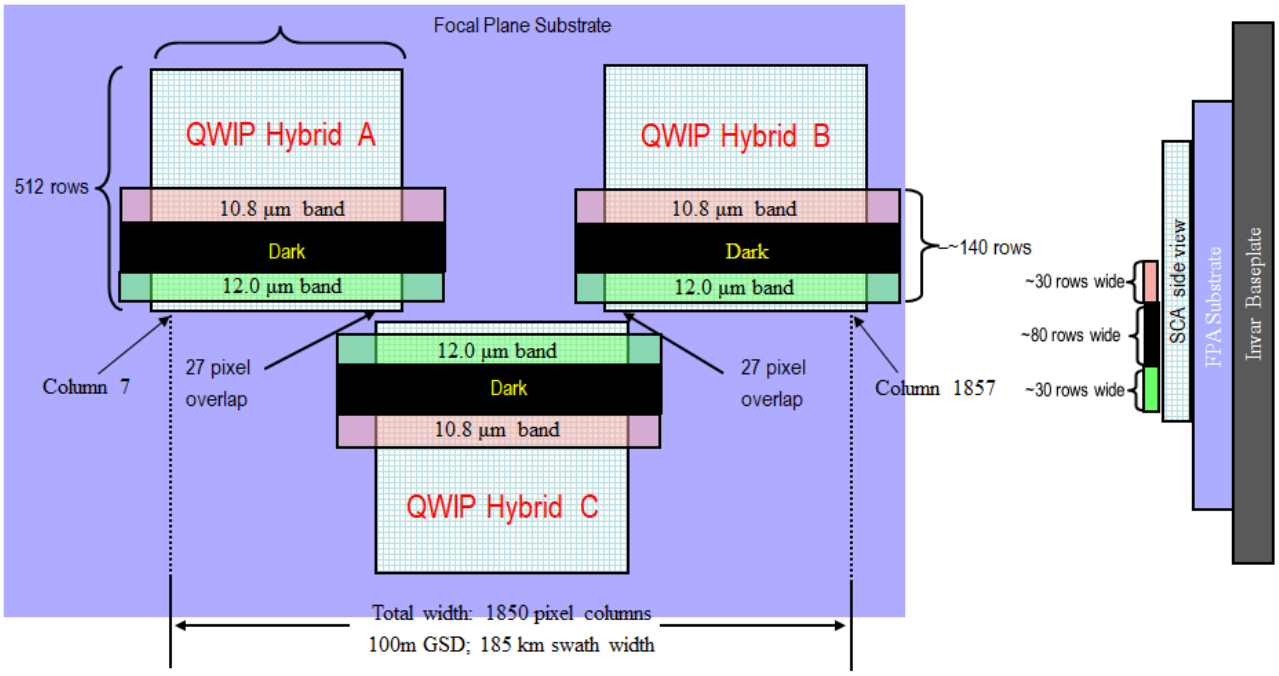

Figure 1. General FPA and Filter layout.

The FPA has three different pixel bands; 12.0μm, 10.8μm, and dark. To achieve these three different bands, a filter holder with six stick filters (three 12.0um filter and three 10.8um filters) is installed above the three QWIP detectors. This can also be seen in Figure 1. Each filter covers about 60 rows but there are 30 un-vignetted rows per filter that we choose the science rows from.

There are a number of level 5 FPA requirements that determine whether or not a pixel or row of pixels is considered a science pixel. These requirements are listed below.

- Within each filter band on each SCA, the FPA shall provide at least 3 unique pixel rows which can be combined through ground processing so that any combination of 2 rows have fewer than 0.1% of the pixel elements that fail to meet operability requirements for any continuous data collection period up to 44 minutes.

- Read noise shall be less than 1000 electrons.

- At the nominal operating temperature of 43 K, the FPA shall have a combination of Conversion Efficiency and Dark Current such that the predicted (NEΔT) for the 10.8 micron band with a 300 K target is less than 0.33 K. The predicted NEΔT will be calculated using the TIRS radiometric noise model assuming all other values in the noise calculation are at their acceptance values.

- At the nominal operating temperature of 43 K, the FPA shall have a combination of the minimum Conversion Efficiency (CE) and Dark Current (ID) such that the predicted (NEΔT) for the 12.0 (11.5-12.5μm) micron band with a 300 K target is less than 0.33 K. The predicted NEΔT will be calculated using the TIRS radiometric noise model assuming all other values in the noise calculation are at their acceptance values.

- Full well capacity shall be greater than 5 million e-
- Dark current variation at nominal stable operating conditions must be <5.1E5 e-/s over 44 min
- The Conversion Efficiency shall be stable to less than 0.4% (peak to peak) of the mean over 44 minutes and shall be stable to less than 0.15% (RMS) of the mean over 35 seconds at nominal stable operating conditions.

Analysis is performed on a per pixel basis for all of these requirements. Any pixel failing any of these requirements will be flagged as nonfunctional. Once the full nonfunctional pixel mask has been created, perfect rows can be determined. As stated in the first requirement listed, the FPA needs one row or combination of two adjacent rows that meets all of the science pixel requirements for each of the three bands (12.0um, 10.8um, dark). These rows, or combination of rows, are considered 'perfect rows'. The following sections show the individual test analysis as well as the nonfunctional pixel and 'perfect row' determinations.

3. TEST RESULTS

3.1 Dark Current

Dark images were collected with detector bias voltages of 0.2V, 0.4V, 0.6V, 0.8V, and 1V at each of the following QWIP temperatures: 37K, 38K, 39K, 41K, 43K, 45K, and 47K. Dark current files with several different integration times were used in order to measure the signal vs. exposure time for each QWIP array. Figure 2 shows a dark current difference image between exposures of 20ms and 30ms at a bias voltage of 0.6V, and detector temperature of 43K.

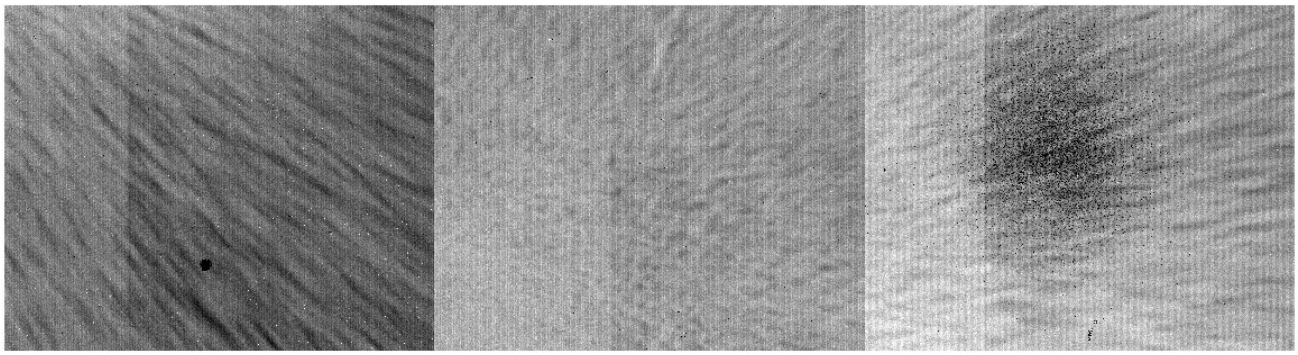

Figure 2. Dark image resulting from the difference of 20ms and 30ms dark exposures. Darker areas in the image indicate lower dark current. From left to right: Q253 (A), Q249 (B), and Q254 (C).

The dark current is measured by acquiring frames with several different exposure times and plotting the dark signal versus exposure time. An example of this is shown in Figure 3. Careful analysis reveals two separate regions where the dark increases linearly with exposure time. We attribute this to a change in gain with signal that is expected to occur for the 9803 ROICs where the integrating capacitor changes by a factor of approximately 3 at about 11 percent of full well. Avoiding the transition region, we fit two lines, one at high signals assuming a gain of 151 electrons/ADU based on a node capacitance of 0.55pF on the 9803 input amplifier (effective integrating capacitance) and one at low signals assuming a gain of 40.5 electrons/ADU (i.e. approximately 1/3 of the high gain case). These separate measurements yield the same dark current rate to within about 5 percent. Figure 4 maps the high signal dark current as a function of bias voltage at different temperatures.

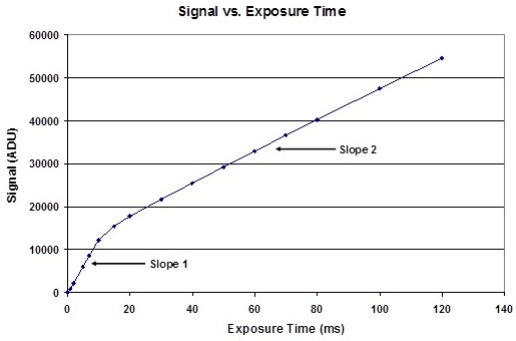

Figure 3. An example of transition in signal accumulation for the 9803 ROIC.

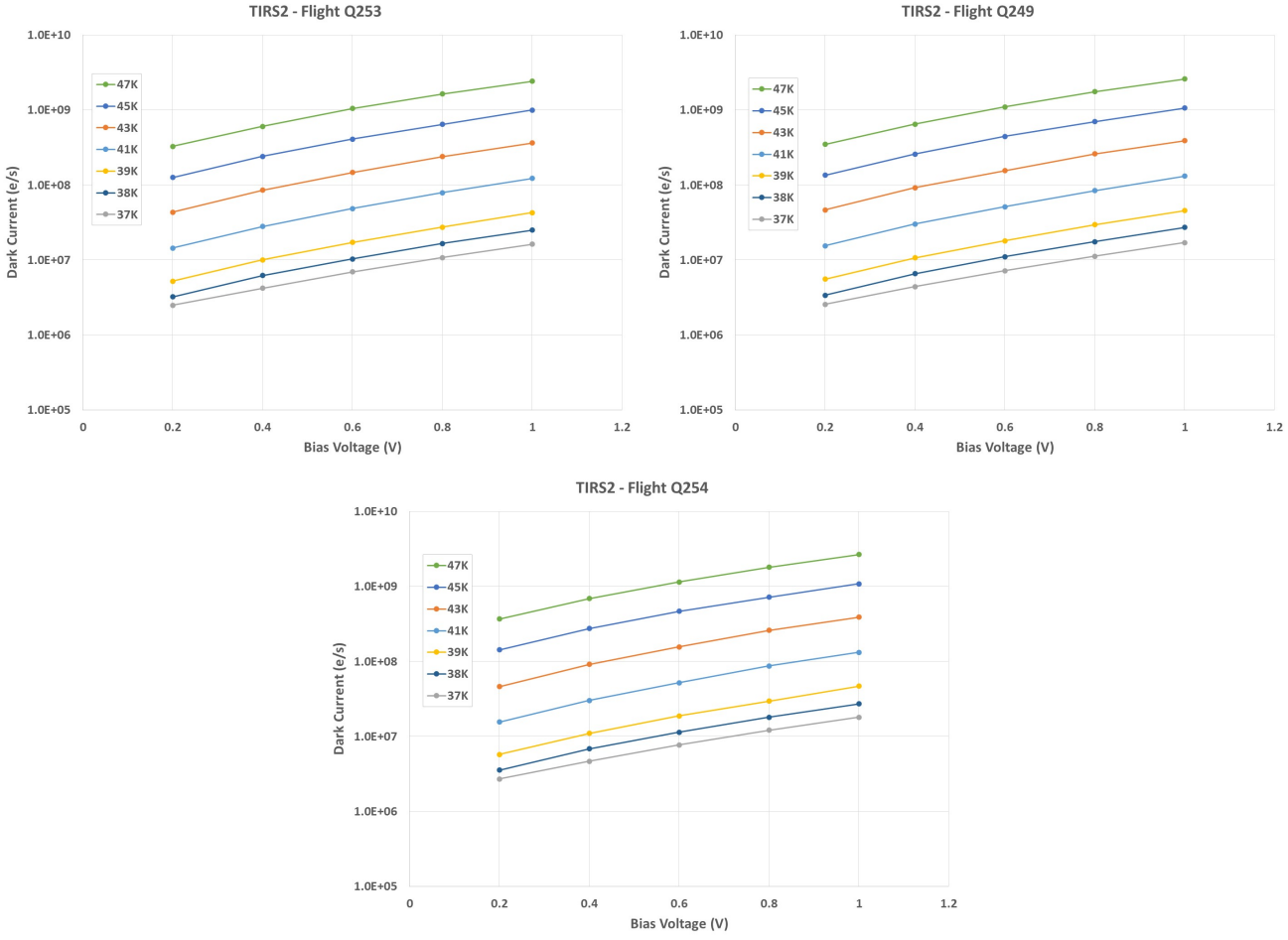

Figure 4. Dark current for Q253 (top left), Q249 (top right), and Q254 (bottom) at multiple temperatures and bias voltages.

3.2 Noise

The FPA read noise was measured by obtaining the standard deviation of a difference of short (100μs) dark exposures at a detector temperature of 43K for each detector. By taking the difference of two short dark exposure frames, the pixel-to-pixel CE nonuniformity and dark current effects are reduced. The standard deviation of the resulting difference frame is calculated and then divided by $\sqrt{2}$ in order to get the readout noise for a single read. The read noise does not vary much on a pixel to pixel level, so the standard deviation for the array is representative of the per pixel read noise. As seen in Table 1 below, the noise for the array increases with an increase in bias voltage. This increase in noise is expected because the dark current signal, and therefore the dark shot noise, increases with bias voltage. The numbers quoted below have not been corrected for the dark shot noise and should therefore be viewed as an upper limit of the read noise. Because the noise was calculated from files with a very low signal level (under 1000 ADU), a gain of 40.5 e-/ADU was applied.

Table 1. Detector read noise vs. bias

Bias Voltage (Volts)	Q253 (A) Read Noise (e-)	Q249 (B) Read Noise (e-)	Q254 (C) Read Noise (e-)
0.2	255	251	274
0.4	268	262	285
0.6	273	267	290
0.8	267	259	287
1.0	264	258	287

In order to calculate the noise per pixel, a short dark exposure of 100 μs containing 100 frames is collected. The standard deviation per pixel over the 100 frames is multiplied by a conversion gain of 40.5 electrons per ADU since the signal is within the first slope (seen in Figure 3). If a pixel has a noise value exceeding 1000 electrons it is considered nonfunctional. The results for a bias voltage of 0.6V are displayed as a histogram in Figure 5. Using the threshold of 1000 electrons, there are 10 total pixels (out of 983,040 pixels) that do not meet this requirement (0 in Q253 (A), 6 in Q249 (B), and 4 in Q254 (C)).

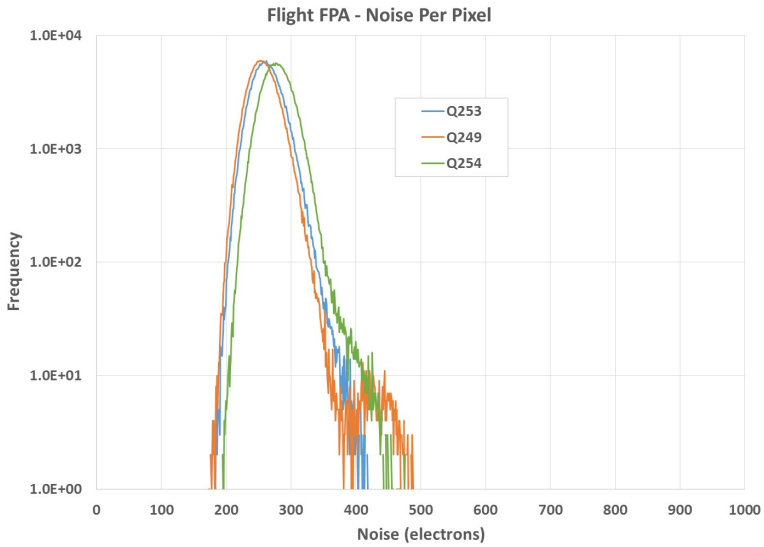

Figure 5. Noise per pixel histogram for each array in the flight FPA at 0.6V bias.

3.3 Dark Current Stability

In order to assess the stability of the dark current over a 45-minute period, a set of four dark images of varying exposure times are collected every two minutes for a total of 23 sets. This test is performed at a detector temperature of 43K. Dark current per pixel is calculated for each set in electrons per second (a gain of 151 e-/ADU was applied since all images collected fall within the second slope of Figure 3.) To calculate change in dark current, we measured the maximum and minimum dark current values for every pixel over the 45-minute period, i.e., peak-to-peak change of dark current. In order to successfully meet the requirement the dark current should change by no more than 5.1×10^5 e/s based on the calculation:

$$\Delta Idark \leq 7 \times 10^8 \times 0.002 \times 2 \div 5.5 \equiv 5.1 \times 10^5$$

This threshold is derived from the TIRS Noise Model and project specifications for maximum dark current. The project specifies that the maximum dark current change over 45 minutes should be no more than 0.2% of the maximum allowable dark current of 7×10^8 e-/s for a 2ms integration time. We use the TIRS Noise Model to calculate Noise Equivalent delta Temperature (NEΔT), a parameter from which we derive operating dark current and conversion efficiency thresholds for nonfunctional pixel analysis, and the model bases its calculations on an integration time of 5.5ms. To find the appropriate maximum dark current change for our noise model, we scale the maximum dark current change from the project specifications of 2ms to our operating exposure time of 5.5ms (see equation above).

In the focal plane, there are a total of 5 pixels whose peak-to-peak instability exceeds 5.1×10^5 e/s (0 in Q253 (A), 1 in Q249 (B), and 4 in Q254 (C)). The peak-to-peak change in dark current over the 45-minute period for each pixel is shown in Figure 6, where lighter pixels indicate higher dark current instability.

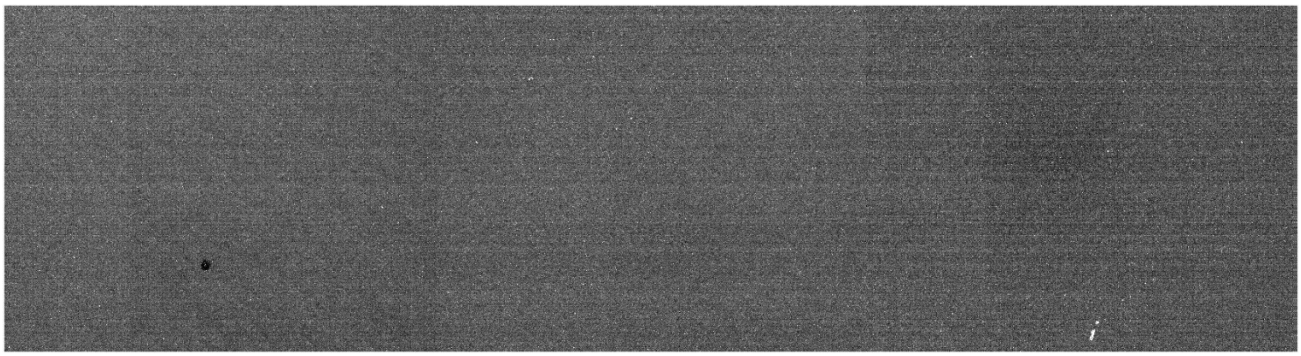

Figure 6. The peak-to-peak change in dark current per pixel over the 45-minute period (lighter pixels have a larger change in dark current.) Left to right: Q253 (A), Q249 (B), Q254 (C).

3.4 Conversion Efficiency Stability

The stability of the conversion efficiency is assessed by exposing the detector array to a 315K black body and monitoring the changes in conversion efficiency. The black body is placed under vacuum in order to minimize any black body temperature fluctuations due to changes in the surrounding environment. Ninety frames are collected every 90 seconds. These ninety frames comprise an image set. Over a period of 45 minutes, a total of 30 image sets are collected. For each image set, the first of the 90 frames (which is a 34μs baseline image) is averaged over all pixels for a mean baseline value. The following 89 frames are averaged pixel-by-pixel, resulting in a single average image. The mean baseline value is subtracted from its corresponding image to obtain the change in signal for each pixel. A pixel whose peak-to-peak change in CE exceeds 0.4% of the mean integrated signal over the 45-minute period is considered nonfunctional.

In the focal plane, there are a total of 2403 pixels whose peak-to-peak instability exceeds 0.4% of the integrated signal (230 for Q253 (A), 49 for Q249 (B), and 2124 for Q254 (C)). If we only include the pixels in the three

science bands, the number of pixels with high CE instability drops to 338 (6 for Q253 (A), 7 for Q249 (B), and 325 for Q254 (C)). The peak-to-peak change in conversion efficiency over the 45-minute period for each pixel is shown in Figure 7; lighter pixels have greater CE instability.

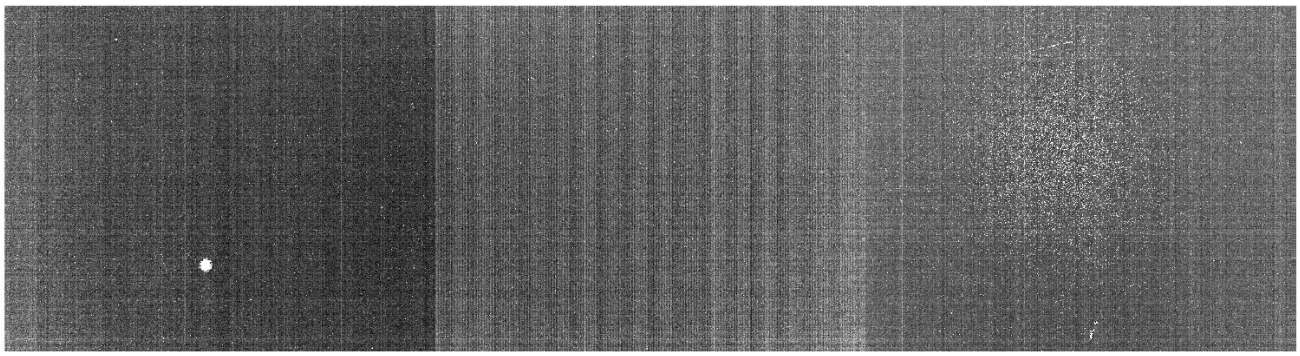

Figure 7. The peak-to-peak change in response as a percentage of integrated signal over 45 minutes (lighter pixels indicate greater CE instability). Left to right: Q253 (A), Q249 (B), and Q254 (C).

Similar to the 45-minute CE stability test, another CE stability test is performed over 35 seconds. While exposed to the same 315K black body used in the 45-minute stability test, an image set comprised of 251 frames is collected. An integration time is chosen to collect a total of roughly 5 million electrons. The first of the 251 frames is averaged over the entire array to get a global background signal. This value is subtracted from the subsequent 250 frames in order to calculate the total signal per pixel. The 250 frames are then averaged into 10, 25-frame images. The standard deviation per pixel over the 10 averaged frames is calculated and divided by the mean signal per pixel. A pixel whose change in CE is greater than 0.15% RMS is identified as a nonfunctional pixel. For the focal plane, there are 463 total pixels that do not meet the 0.15% RMS requirement (43 in Q253 (A), 18 in Q249 (B), and 402 in Q254 (C)). In the science bands, there are a total of 52 (3 in Q253 (A), 3 in Q249 (B), and 46 in Q254 (C)). Figure 8 shows the CE stability over 35 seconds per pixel (the lighter pixels have a higher instability).

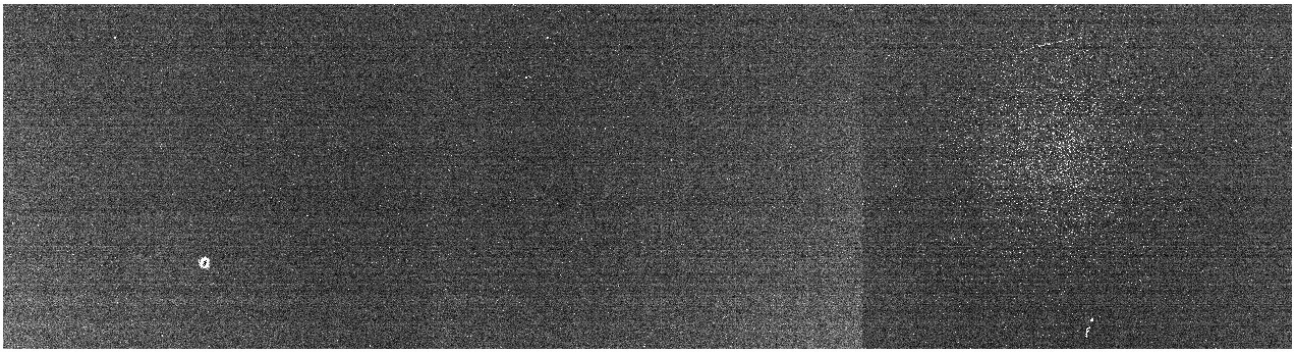

Figure 8. A map of CE stability using a 35-second data set (lighter pixels indicate greater CE instability). Left to right: Q253 (A), Q249 (B), and Q254 (C).

3.5 Power Dissipation

The detector voltages were measured for a detector bias voltage of 0.6V with third generation Leach electronics operating in 4-channel mode. The results for each array can be seen in Tables 2, 3, and 4 below.

Table 2. Power Dissipation for Q253, Detector Bias of 0.6V

Bias Line	Supply side	Load side	Resistor	Current Load	Power Dissipation
Vdetcom	6.017 V	6.000 V	110 Ω	0.15 mA	0.90 mW
Vref	1.614 V	1.614 V	0 Ω	0.00 mA	0.00 mW
Vpd	5.597 V	5.592 V	10 Ω	0.50 mA	2.80 mW
Vpos	5.602 V	5.492 V	10 Ω	11.3 mA	62.0 mW
Vposout	5.603 V	5.456 V	10 Ω	15.1 mA	82.3 mW
TOTAL					148 mW

Table 3. Power Dissipation for Q249, Detector Bias of 0.6V

Bias Line	Supply side	Load side	Resistor	Current Load	Power Dissipation
Vdetcom	6.011 V	5.996 V	110 Ω	0.14 mA	0.84 mW
Vref	1.614 V	1.614 V	0 Ω	0.00 mA	0.00 mW
Vpd	5.597 V	5.576 V	10 Ω	2.10 mA	11.71 mW
Vpos	5.602 V	5.492 V	10 Ω	11.0 mA	60.4 mW
Vposout	5.603 V	5.456 V	10 Ω	14.7 mA	80.2 mW
TOTAL					153 mW

Table 4. Power Dissipation for Q254, Detector Bias of 0.6V

Bias Line	Supply side	Load side	Resistor	Current Load	Power Dissipation
Vdetcom	6.025 V	6.004 V	110 Ω	0.19 mA	1.14 mW
Vref	1.614 V	1.614 V	0 Ω	0.00 mA	0.00 mW
Vpd	5.597 V	5.592 V	10 Ω	0.50 mA	2.80 mW
Vpos	5.602 V	5.495 V	10 Ω	10.7 mA	58.8 mW
Vposout	5.603 V	5.455 V	10 Ω	14.8 mA	80.7 mW
TOTAL					143 mW

3.6 Spectral Response

Relative CE measurements are collected using a SpectraPro 300i monochromator, a 995C blackbody source, and order sorting filters with cut-ons at 1.6, 2.7, 5.4, 6.0, 9.0, and 10.5 μm. The out-of-band (2-7.5μm, 14-20μm) relative spectral response was measured at the FPA level for each SCA by opening the cold shutter and exposing the SCA to a partial flat field illumination from a blackbody radiation source.

Spectral power distribution at the monochromator output is measured with a calibrated model FTIR16-2 HgCdTe detector whose absolute accuracy is about 5% at each wavelength. At each wavelength, the output of the monochromator is measured with the calibrated detector and with the QWIP. The QWIP output value is compared to the calibrated detector measurement to provide a calibrated relative response at each wavelength. This process does not correct for the effect of atmospheric transmittance, however this is negligible over the short path lengths used in the measurements. The test dewar window transmission was taken into account. The equation used to calculate the relative response is:

Relative Response = Raw median detector counts above background / HgCdTe relative response / HgCdTe measured response / Wavelength

The relative spectral response for each QWIP can be seen in Figure 9. The absolute conversion efficiency was

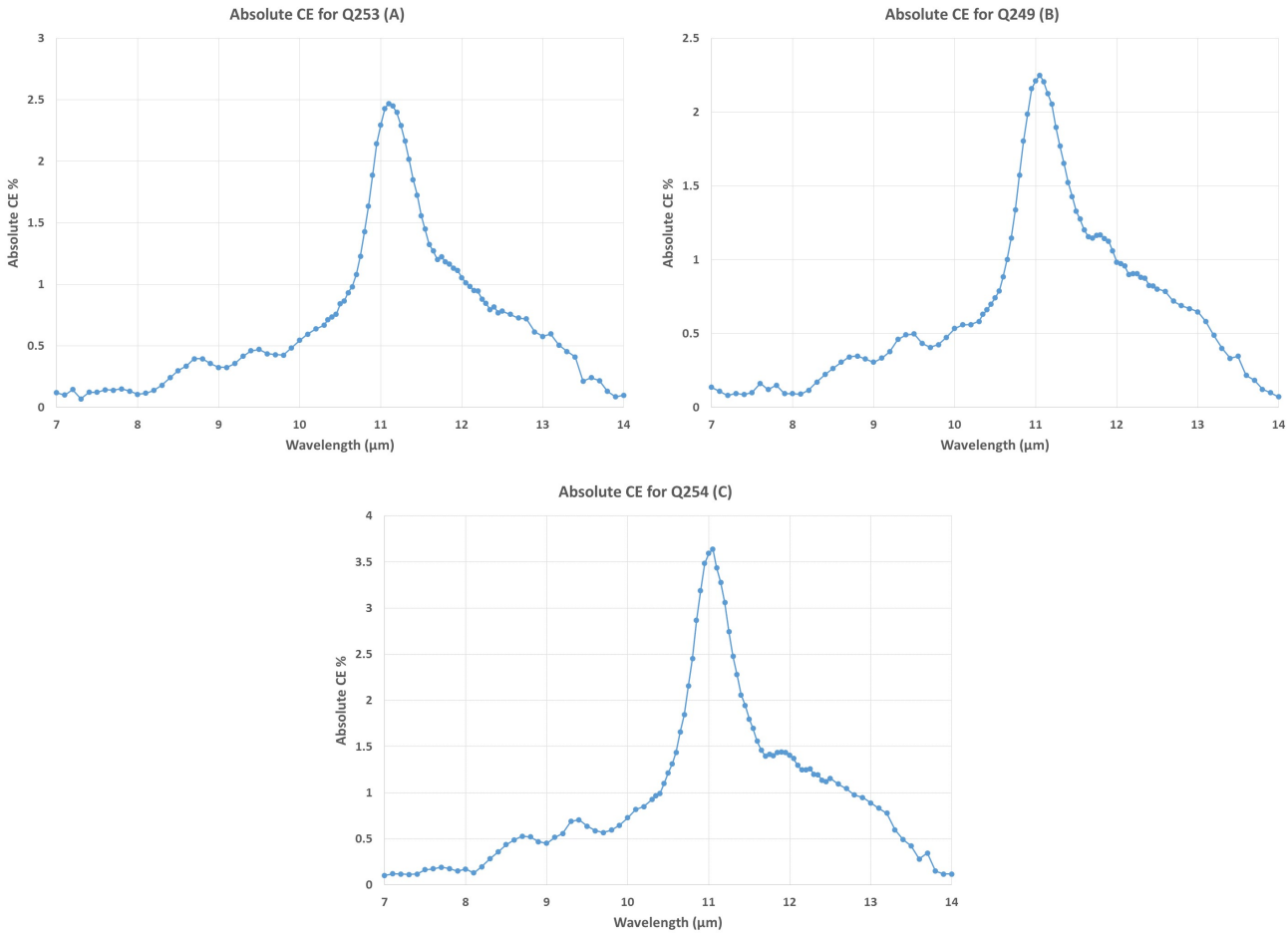

Figure 9. Absolute Spectral Response for Q253 (top left), Q249 (top right), and Q254 (bottom).

measured for each device at the SCA level and the peak responses were: 2.47% for Q253 (A), 2.25% for Q249 (B), and 3.64% for Q254 (C).

3.7 Noise Equivalent Delta Temperature (NEΔT)

The specific dark current and CE limits used for each SCA are based on the TIRS project noise model by assessing which bias voltage was optimal for high functional pixel and functional row yield. Operating the detector at a bias voltage of 0.60V proved optimal for yielding a minimal number of nonfunctional pixels. For Q253 (A), we define a hot pixel as having a dark rate greater than 2.463×10^8 electrons per second, and a low CE pixel as having a conversion efficiency response less than 0.68% anywhere between 10.5-12.3μm. For Q249 (B), the thresholds are 2.166×10^8 electrons/second and 0.6% CE. For Q254 (C), the thresholds are 2.166×10^8 electrons/second and 0.6% CE.

3.8 Nonfunctional Pixels

We combine NEΔT, 45-minute dark current stability, 45-minute conversion efficiency instability, 35-second conversion efficiency stability, and noise per pixel criteria to find all nonfunctional pixels. A summary of nonfunctional pixels can be seen for each SCA in Tables 5, 6, 7. Each criterion used to determine nonfunctional pixels is independent of one another, so there are pixels that may be categorized as nonfunctional by more than one criterion.

Table 5. Q253 (A) nonfunctional pixels not meeting NEΔT and stability requirements.

Type of Pixel	Thresholds	Total Numbers of Pixels	% of Area
Hot	Idark > 2.463×10^8 e-/s	30	<0.1
Low CE	CE < 0.68%	283	<0.1
Unstable Dark Current	Change in Idark > 5.1×10^5 e-/s over 45 minutes	0	0.0
Unstable CE	Change in CE > 0.4% of mean integrated signal over 45 minutes	230	<0.1
High Noise	Noise > 1000 e-	0	0.0
Short-Term Unstable CE	Change in $CE > 0.15\%$ (RMS) of mean integrated signal over 35 seconds	43	<0.1
Total Nonfunctional Pixels	NEΔT > 0.39K	385	0.11
Total Functional Pixels	NEΔT $\leq$ 0.39K	327295	99.89

Table 6. Q249 (B) nonfunctional pixels not meeting NEΔT and stability requirements.

Type of Pixel	Thresholds	Total Numbers of Pixels	% of Area
Hot	Idark > 2.166×10^8 e-/s	38	<0.1
Low CE	CE < 0.6%	94	<0.1
Unstable Dark Current	Change in Idark > 5.1×10^5 e-/s over 45 minutes	1	<0.1
Unstable CE	Change in CE > 0.4% of mean integrated signal over 45 minutes	49	<0.1
High Noise	Noise > 1000 e-	6	<0.1
Short-Term Unstable CE	Change in $CE > 0.15\%$ (RMS) of mean integrated signal over 35 seconds	18	<0.1
Total Nonfunctional Pixels	NEΔT > 0.39K	152	0.05
Total Functional Pixels	NEΔT $\leq$ 0.39K	327528	99.95

Table 7. Q254 (C) nonfunctional pixels not meeting NEΔT and stability requirements.

Type of Pixel	Thresholds	Total Numbers of Pixels	% of Area
Hot	Idark > 2.166×10^8 e-/s	73	<0.1
Low CE	CE < 0.6%	105	<0.1
Unstable Dark Current	Change in Idark > 5.1×10^5 e-/s over 45 minutes	4	<0.1
Unstable CE	Change in CE > 0.4% of mean integrated signal over 45 minutes	2124	0.65
High Noise	Noise > 1000 e-	4	0.0
Short-Term Unstable CE	Change in $CE > 0.15\%$ (RMS) of mean integrated signal over 35 seconds	402	0.12
Total Nonfunctional Pixels	NEΔT > 0.39K	2281	0.70
Total Functional Pixels	NEΔT $\leq$ 0.39K	325399	99.30

Figure 10. Map of all nonfunctional pixels (in blue) not meeting NEΔT, stability, or noise thresholds. Left to right: Q253 (A), Q249 (B), and Q254 (C).

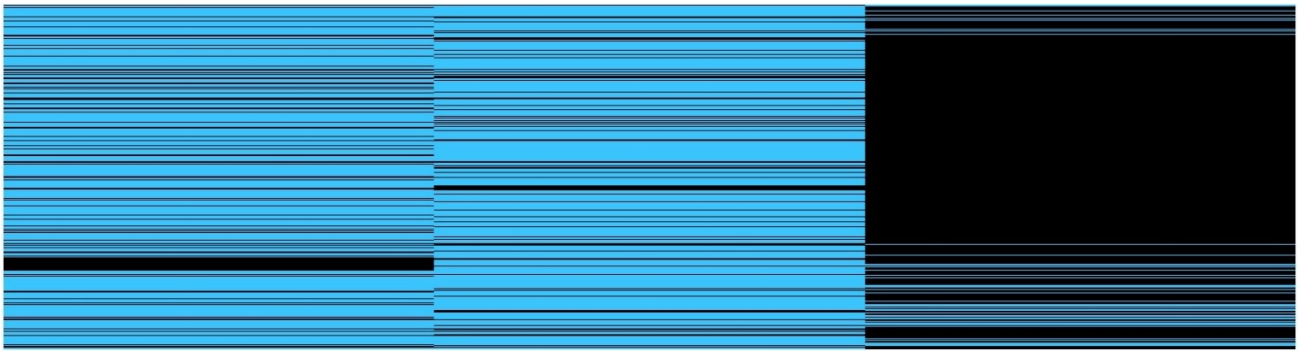

Figure 11. Map of perfect rows. Blue rows have no inoperable pixels. Left to right: Q253 (A), Q249 (B), and Q254 (C).

Since there are 2 out of 9 science bands with no perfect rows, it was important to evaluate the possibility of combining rows in order to form rows with no inoperable pixels. For the analysis in this report, the only combinations that were studied used neighboring rows. For example, if row number 400 can be combined with either row 399 or row 401 to yield no inoperable pixels, number 400 is considered to be good in the combination analysis. Table 8 and Figure 12 summarize the results using combinations of neighboring rows.

Table 8. Summary of perfect rows and rows that can be combined with neighboring rows to form rows with no inoperable pixels.

	Q253 (A)		Q249 (B)		Q254 (C)	
Band	Perfect	Perfect (with combinations)	Perfect	Perfect (with combinations)	Perfect	Perfect (with combinations)
Top	26/30	30/30	24/30	30/30	6/30	30/30
Middle	19/22	22/22	18/22	22/22	0/22	22/22
Bottom	22/30	30/30	24/30	30/30	0/30	29/30

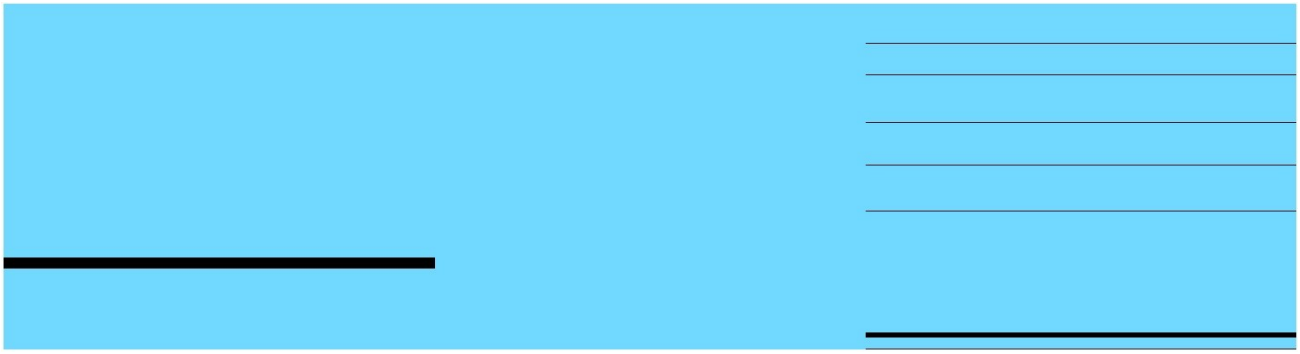

Figure 12. Map of rows that can be combined with a neighboring row to form a row with no inoperable pixels (shown in blue). Left to right: Q253 (A), Q249 (B), and Q254 (C).

4. CONCLUSION

After testing and analysis at the TIRS-2 subsystem level, the flight FPA was found to meet all level 5 requirements. The flight filter was then installed to the flight FPA by engineers at the DCL. Once the FPA assembly with flight filter was delivered to TIRS-2 integration and testing it was integrated to the flight telescope. The entire flight telescope assembly went through two rounds of thermal vacuum testing to adjust the FPA tip and tilt. After meeting the requirements of the telescope thermal vacuum testing the telescope assembly was integrated into the flight instrument structure and is currently awaiting instrument level testing as NASA GSFC.

ACKNOWLEDGMENTS

The author would like to thank the following people for their support on the NASA Landsat 9/TIRS-2 Instrument: Augustyn Waczynski, Duncan Kahle, Eric Kan, Jim Williams, Allen Lunsford, Joel McCorkel, Aaron Perlman, Boryana Efremova, Andrew Uhl, FLIR, Qmagiq, LLC, and all Landsat 8/TIRS FPA engineers.

REFERENCES

[1] J. Hair, e. a., "Landsat 9 thermal infrared sensor 2 architecture and design," *IGARSS* (2018).

[2] M. Jhabvala, e. a., "Performance of the qwip focal plane arrays for nasa's landsat data continuity mission," *Proc. SPIE* **8012**, Infrared Technology and Applications XXXVII (80120Q (20 May 2011)).

[3] D. Reuter, e. a., "The thermal infrared sensor on the landsat data continuity mission," *2010 IEEE International Geoscience and Remote Sensing Symposium*, pp. 754–757 (2010).